Received: 2 March 2023 | Revised: 29 September 2023 | Accepted: 10 October 2023

DOI: 10.1111/ejss.13426

RESEARCH ARTICLE

European Journal of Soil Science WILEY

Fifty years after deep-ploughing: Effects on yield, roots, nutrient stocks and soil structure

Dymphie J. Burger[1] | **Florian Schneider**[2] | **Sara L. Bauke**[1] | **Timo Kautz**[3] | **Axel Don**[2] | **Wulf Amelung**[1]

[1]Institute of Crop Science and Resource Conservation (INRES)-Soil Science and Soil Ecology, University of Bonn, Bonn, Germany

[2]Thünen Institute of Climate Smart Agriculture, Braunschweig, Germany

[3]Department of Agronomy and Crop Science, Faculty of Life Sciences, Humboldt University Berlin, Berlin, Germany

Correspondence
Dymphie J. Burger, Institute of Crop Science and Resource Conservation (INRES)-Soil Science and Soil Ecology, University of Bonn, Nussallee 13, 53115 Bonn, Germany.
Email: dburger@uni-bonn.de

Funding information
BonaRes, Grant/Award Numbers: 031B0151A, 031B0151E, 031B0151G

Abstract

Deep-ploughing far beyond the common depth of 30 cm was used more than 50 years ago in Northern Germany with the aim to break root-restricting layers and thereby improve access to subsoil water and nutrient resources. We hypothesized that effects of this earlier intervention on soil properties and yields prevailed after 50 years. Hence, we sampled two sandy soils and one silty soil (Cambisols and a Luvisol) of which half of the field had been deep-ploughed 50 years ago (soils then re-classified as Treposols). The adjacent other half was not deep-ploughed and thus served as the control. At all the three sites, both deep-ploughed and control parts were then conventionally managed over the last 50 years. We assessed yields during the dry year 2019 and additionally in 2020, and rooting intensity at the year of sampling (2019), as well as changes in soil structure, carbon and nutrient stocks in that year. We found that deep-ploughing improved yields in the dry spell of 2019 at the sandy sites, which was supported by a more general pattern of higher NDVI indices in deep-ploughed parts for the period from 2016 to 2021 across varying weather conditions. Subsoil stocks of soil organic carbon and total plant-available phosphorus were enhanced by 21%–199% in the different sites. Root biomass in the subsoil was reduced due to deep-ploughing at the silty site and was increased or unaffected at the sandy sites. Overall, the effects of deep-ploughing were site-specific, with reduced bulk density in the buried topsoil stripes in the subsoil of the sandy sites, but with elevated subsoil density in the silty site. Hence, even 50 years after deep-ploughing, changes in soil properties are still detectable, although effect size differed among sites.

KEYWORDS

aggregates, carbon sequestration, deep-ploughing, macronutrients, subsoil, Treposol

1 | INTRODUCTION

In recent years, crop yields in Central Europe and other parts of the world have been increasingly limited by summer drought periods (Peters et al., 2020; Toreti et al., 2019). Due to soil drying, inorganic forms of nutrients that are usually readily available in the soil solution can thus not move through the soil matrix (Amtmann & Blatt, 2009), which affects crop growth via both the lack of water and subsequent impaired nutrient uptake (Querejeta et al., 2021). A large part of soil macronutrients, including nitrogen (N), phosphorus (P) and potassium (K), however, is stored below the plough pan, in the subsoil (Kautz et al., 2013), which thus becomes an attractive option to plants. In a similar manner, also Querejeta et al. (2021) found that under topsoil drying, shrubs took up more water and nutrients from the subsoil than before, so that subsoil water and nutrient reserves compensated for respective limitations in the topsoils during dry spells (Querejeta et al., 2021). However, this reserve of nutrients is not always accessible for plants due to root-restricting layers (Schneider & Don, 2019a). Such root-restricting layers originate from both compaction by heavy machinery (Gao et al., 2016), and, likely even more frequently, from pedogenetic or geologic hardpans, including densely packed and cemented horizons as well as occurrences of rock fragments or abrupt textural changes (Schneider et al., 2017; Schneider & Don, 2019a). Due to the lower amount of macropores in these dense layers, the connectivity and continuity of the pore system is disrupted (Berisso et al., 2013), which can lead to anisotropy of the saturated hydraulic conductivity (Ksat) (Beck-Broichsitter et al., 2020) and can affect root growth and root anatomy (Lipiec et al., 2012). This both limits water and nutrient uptake by plants and thus results in lower crop yields (Lipiec et al., 2012; Schneider & Don, 2019a).

To avoid such yield losses, there are several ways to break root-restricting layers, for example, by choosing deep-rooting crops or pre-crops (Perkons et al., 2014; Schneider & Don, 2019b), promoting the formation of biopores by earthworms (Kautz et al., 2013), or via physical amelioration measures like drainage, deep loosening, or deep-ploughing (Schneider & Don, 2019b). The latter turns the soil horizons so that a part of the subsoil is exposed at the soil surface and parts of the topsoil are buried (Schneider et al., 2017).

The term deep-ploughing is used in this study as a one-time, deep, physical modification of the soil profile with the aim of long-term soil melioration, in contrast to annual ploughing, which aims at seedbed preparation, residue incorporation and weed control (Alcantára et al., 2016). Many deep-ploughed sites in northwest Germany near the Dutch-German border resulted from the 'Emslandplan' enacted after World War II to convert the underlying podzols of heathland and drained peatland into agricultural land (Schneider & Don, 2019b). Deep-ploughing was also common in wine-growing regions along the Rhine and Mosel rivers in Germany. In total, approximately 5% of German agricultural land was deep-ploughed (Schneider & Don, 2019b). To this day, the respective soils show remnants of the former topsoil that was partly mixed in strips into the subsoil and vice versa. Therefore, in Germany, these soils have been attributed to a separate classification level (Treposol according to German classification KA5, hortic Anthrosols according to IUSS-WRB, 2015). Deep-ploughing is less popular now but is still used occasionally to break up plough pans under the topsoil horizon.

Positive effects of deep-ploughing include increased soil organic carbon (SOC) stocks due to burial of SOC in the subsoil, particularly in sandy subsoil (Alcantára et al., 2016). Since this SOC was also more stable against decay than SOC in the topsoil and additional SOC accumulated in the 'new' topsoil, an average increase of 42% in stocks was found 35–50 years after deep-ploughing (Alcantára et al., 2017). Additionally, with the former subsoil material being brought to the soil surface, increased SOC sequestration has been observed in the topsoil due to a high amount of uplifted unsaturated mineral particles including Fe and Al oxides that bind SOC (Alcantára et al., 2017; Shen et al., 2021). The elevated amounts of SOC in the subsoil may promote also subsoil aggregation and can maintain lower bulk density and should also provide additional supply of plant-available nutrients (Ponder, 1981; Sharpley, 2003). In combination, these effects thus finally support root development and crop performance, particularly when subsoil water and nutrient reserves are needed to overcome years with drought stress (Izumi & Wagai, 2019). By contrast, negative impacts of deep-ploughing include disruption of the aggregates and soil structure, leading to higher risks of erosion by wind and rainfall, and to losses of SOC

Highlights

- Deep tillage maintained differences in soil properties after 50 years.
- Effects were site-specific, yield was higher at the sandy sites in the dry year 2019.
- Subsoils had higher aggregate-soil organic carbon stocks after deep tillage.
- Deep tillage had homogenized nutrient distributions in the soil profile.

(Zhao et al., 2018). Especially in fine-textured soils that can maintain high soil moisture content, deep-ploughing can facilitate soil compaction after the ploughing event and therewith finally limit crop growth (Botta et al., 2006). Besides, there is the risk of diluting topsoil fertility with subsoil material, while vice versa the inclusion of topsoil material into the subsoil will enhance subsoil fertility. Yet, soil structural, soil biochemical, root growth and yield parameters have never been assessed together more than 50 years after deep-ploughing, particularly not for differently textured soils, thus making it difficult to identify the underlying mechanisms of site- and soil texture-specific long-term effects of deep-ploughing on crop development.

The objective of this study was to test the hypotheses that (i) deep-ploughed soils maintain elevated yields in a dry year and are supported by elevated root growth in the subsoil, which is accompanied by (ii) elevated amounts of macroaggregates in the buried topsoil stripes, as well as by (iii) elevated stocks of SOC, total N and plant-available P and K. As such effects may be site-specific, we sampled sites with divergent soil texture and with and without deep-ploughing during a year with summer drought, and assessed yield differences, soil aggregation, and soil macro- and micronutrient stocks.

2 | METHODS

2.1 | Site descriptions

Three formerly deep-ploughed cropland sites were selected for this study in Banteln (haplic Luvisol), Elze, and Essemühle (both dystric Cambisols) in Lower Saxony, northwestern Germany; the site characteristics are described in Table 1. Each field site consisted of a deep-ploughed part of around 200 m length (hortic Anthrosols [Relocatic] according to IUSS-WRB, 2015; Treposol according to the German soil classification system) and an adjacent non-deep-ploughed reference part of the same size

TABLE 1 Site characteristics, mean annual precipitation and temperature, and cropland management during the previous 10 years (2004–2014) adapted after (Alcantára et al., 2016, 2017).

	Banteln	Elze	Essemühle
Site property			
Location (degrees minutes seconds)	52°05′13″ N 9°44′56″ E	52°35′06″ N 9°45′29″ E	52°45′50″ N 8°28′34″ E
Mean annual precipitation (mm, 1990–2020) (SEM)	628 (19)	628 (19)	689 (23)
Mean annual temperature (°C, 1990–2020) (SEM)	10.0 (0.5)	10.0 (0.5)	9.9 (0.1)
Soil type (IUSS-WRB, 2015)	Haplic Luvisol	Dystric Cambisol	Dystric Cambisol
Parent material	Loess	Pleistocene sand	Pleistocene sand
Sand (%)	5	84	88
Silt (%)	82	12	8
Clay (%)	13	4	4
pH (average ± SEM)	6.6 ± 0.1	5.3 ± 0.1	4.8 ± 0.1
Land management			
Year of deep-ploughing (years since)	1965 (54)	1968 (51)	1968 (51)
Deep-ploughing depth (cm)	85	55	75
Annual ploughing depth (cm)	32	35	27
Crop rotation[a]	SB, w.W, M	w.RS, w.R, P	RS, P, w.B, R, M
Straw removal	No	Partially	Partially
Cover crops	Mustard	Mustard	Oilseed radish
Organic fertilizer application per ha and year[b]	-	2 m^3 ps, 2 Mg pm	16 m^3, cs, 12 m^3 ps, 4 m^3 day, 1 Mg ppl
Mineral N fertilization per ha and year (kg)	201	121	128

Note: The soil management practices were performed on an annual basis, except for the deep-ploughing, which only occurred once.

[a]P, potato; R, rye; RS, oilseed rape; SB, sugar beet; w, winter; W, wheat.

[b]cs, cattle slurry; day, digestate; pm, pig manure; ppl, potato protein liquid; ps, pig slurry.

(Figure S1). Three subplots were set up within each part (Table 1) around 30–80 m away from each other, depending on the size of the field. At each site, the meliorative deep-ploughing intervention occurred only once, in 1965 and 1968 for Banteln, and both Elze and Essemühle, respectively. The topsoil tillage management after that, as well as other management factors, for example, fertilization and crop rotation, was the same for the deep-ploughed and the reference plots with annual ploughing depths of 27–35 cm, also described in Table 1.

Monthly precipitation and air temperature data for the last 30 years were derived from the German Meteorological Service (DWD) station Hannover for both Banteln and Elze (55 m a.s.l., 38 km from Banteln and 31 km from Elze). For Essemühle, the station Diepholz was used, which is 38 m a.s.l. and 22 km away from the site Essemühle. In 2019, mean annual temperature was 11.0°C in Banteln and Elze, and 10.8°C in Essemühle; this is around 1°C higher than the 30-year average (1990–2020) and can therefore be classified as a warmer year. Average precipitation in Banteln and Elze during the last 30 years averaged 628 mm but was 582 mm in 2019. In Essemühle, precipitation in 2019 equalled 734 mm, which was 689 during the reference period (1990–2020), but this site received less precipitation than normal in the first half of 2019.

2.2 | Sampling strategy

2.2.1 | Above-ground biomass sampling and yield estimation

To estimate annual yield during a dry year, above-ground biomass samples (winter wheat in Banteln and rye in Elze and Essemühle) were taken before harvesting, on 20 July 20 2019. At all three locations, 10 samples were taken, five from the deep-ploughed plots and five from the respective adjacent reference plots. The number of ears was determined by counting the number of ears per square meter in the field. The plants were cut off directly above the ground in an area of 50 × 50 cm using battery-powered grass and shrub shears. Fresh weight was determined in the field for each sample. In 2020, plant samples for yield determination were taken similarly as in 2019; however, as potatoes (no cereal crops) were grown in Elze, no samples were taken for yield determination.

In order to prevent microbial decomposition, the plant samples were kept dry in cloth bags until further processing. For estimation of the thousand grain weight, a sample of 1000 grains were separated from the overall biomass sample. To determine the dry mass for grain yield and straw yield, the samples were pooled and then dried at 105°C in a metal bowl for 48 h. Then, the percentage dry matter, grain yield, straw yield, thousand grain weight, and the number of ears were determined. Using the fresh mass (t ha^{-1}) and water content of plant biomass, the average dry matter yield (t ha^{-1}) was calculated.

In order to have a better area representation of the point measurements of the yields at time of plant sampling, as well as to analyse yield data of other years, satellite images from Sentinel 2A and 2B, as well as from Landsat-8 were taken from September 2016 to September 2021 and analysed at a spatial resolution of 10 m. For the sites Banteln and Elze, additional satellite images from September 2021 to September 2022 were used in the analysis. Radiometric correction was conducted with the Framework for Operational Radiometric Correction for Environmental monitoring (FORCE) Level-2 module by Frantz (2019). Using all available satellite images with cloud cover below 75%, monthly normalized difference vegetation indices (NDVI) were calculated for the deep-ploughed plots and reference plots. We assumed that, as NDVI provides information on the photosynthetic biomass during the growing season, it can be used to estimate yield (Durgun et al., 2020; Vannoppen et al., 2020).

2.3 | Root and soil sampling

Root and soil samples were collected in May 2019 during flowering, from all the three sites. At each site, six soil pits of 2–3-m width were excavated. Three pits were located in the reference plot and three pits in the deep-ploughed plot, with the soil pit wall used for root and soil sampling being perpendicular to the ploughing direction. For determining root biomass in and between deep-ploughed topsoil stripes, undisturbed horizontal soil cores were taken in a 10 cm × 10 cm grid at profile walls (Figure 1). The current plough horizon (Ap horizon, 0–30 cm depth) was sampled with seven cores and, depending on the location, 18–28 cores from 30 to 90 cm depth were taken in deep-ploughed plots and 12–18 cores at this depth interval in reference plots. The locations of these cores were selected with the aim to sample both the buried topsoil (rAp, from 30 cm to deep-ploughing depth) and the subsoil (B horizon, 30–90 cm).

These soil cores were stored at 6°C until further processing. A hydropneumatic root washer (GVF, Benzonia, MI, USA) was used to separate roots from soil (Smucker et al., 1982). This system uses a combination of water and air pressure to gently wash out roots in a standardized process described by (do Rosário et al., 2000). After sorting out animals and green plant parts manually, roots were oven-dried at 60°C and weighed to determine root biomass (in mg per cm^3 soil) in the respective depth intervals.

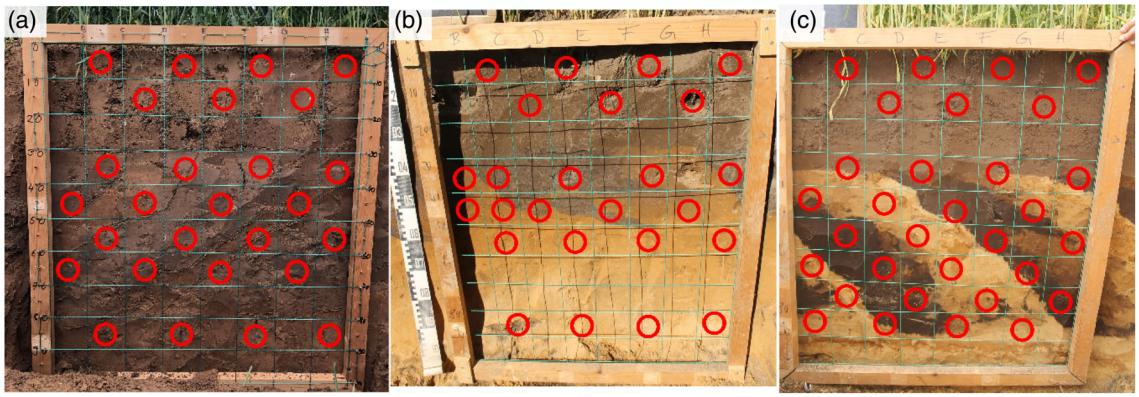

FIGURE 1 Deep-ploughed sites of Banteln (a), Elze (b) and Essemühle (c); with grid for root sampling, the red circles are at the places where the root cores were taken.

The amount of buried topsoil in the samples from the grid was determined by visual assessment of the cells in the root sampling grids. Estimates were then averaged per 10-cm depth interval that was affected by deep-ploughing.

2.4 | Soil structure and bulk density

Samples to determine soil structure parameters were taken per horizon, and the profiles were separated into topsoil (0–30 cm depth), upper (30–50 cm depth) and lower subsoil (50–70 cm depth). The sampling strategy is depicted in Figure S2.

For determining soil structure parameters such as dry bulk density, BD, we adopted the stratified sampling approach of Alcantára et al. (2016). BD was calculated as

$$\mathrm{BD} = m_{\mathrm{tot}}/V_{\mathrm{tot}}, \quad (1)$$

where BD is given in $\mathrm{g\,cm^{-3}}$, V_{tot} is the volume of an undisturbed soil core in $\mathrm{cm^3}$ and m_{tot} is its corresponding mass in g after drying at 105°C until constant weight. Coarse fragments were negligible at all the three sites studied.

For analysis of soil aggregation, in every soil pit, three soil rings with a sample volume of 100 $\mathrm{cm^3}$ per depth interval were used to obtain undisturbed soil samples from sample depths of 20, 40 and 60 cm to correspond with the 0–30 cm, 30–50 cm, and 50–70 cm depths, respectively. The pits of the deep-ploughed plot in Banteln and Essemühle were sampled similarly to the reference plots, adding three extra bulk density rings in the buried topsoil stripes at 40 cm depth to represent the buried topsoil between 30 and 50 cm depth, and three bulk density rings at 60 cm depth in the buried topsoil stripes to represent the 50–70 cm depth, the turned subsoil at this depth interval was not sampled (Figure S2). In Elze, the deep-ploughed plots at 20 and 40 cm depth were sampled the same as those in Banteln and Essemühle. As deep-ploughing did not occur below 50 cm depth at Elze, samples at 60 cm depth were only taken from the subsoil with three bulk density rings. After sampling, the weight of the samples was determined within 48 h and samples were stored at 4°C for soil structure analysis.

The sand proportion, amount of sand-free aggregates and sand-free carbon stock were analysed from the fresh soil samples by wet sieving and sand content correction. The procedure of wet sieving was adapted from (Krause et al., 2018). In brief, prior to wet sieving, 15 g of the undisturbed sample was slowly wetted for 5 min by placing it on a glass fibre filter on the top sieve of the sieving tower at the water surface. Wet sieving was then conducted on a sieving tower with sieves of 2000, 250 and 53 µm mesh size (Retsch® GmbH, Haan, Germany). The sieve tower was moved 3 cm up and down in a water tank for 15 min. The fractions were collected from the sieves by rinsing into a glass flask, frozen and lyophilized (Thermo Fisher Scientific, Waltham, MA, USA). The fraction smaller than 53 µm remained in the bucket and was left to settle overnight after adding a few drops of $MgCl_2$ solution. After that, the water was removed using a water jet pump, and the settled material was collected, frozen and lyophilized as well. Weights of the size fractions were determined, and the size fractions of the field replicates were pooled per site, treatment, depth increment and size fraction, with equal mass of every sample being added to the pooled sample. Small aliquots (0.5 g) of the pooled size fractions were taken for elemental analysis of C and N (vario EL cube, Elementar Analysensysteme GmbH, Langenselbold, Germany).

To correct for sand particles in the same size range as the aggregates, chemical dispersion of the sample was conducted according to Elliot (1991). Every sample

was dispersed with sodium metahexaphosphate (5 g L^{-1} solution) in a sample:solution ratio of 1: 4 (m:v). The samples with solution were shaken overnight and were sieved with a 53 µm sieve to separate the sand and particulate organic matter (POM). The fraction that was larger than 53 µm (sand and POM) was then dried at 50°C and the weight was determined. It was assumed that the POM had such a low density that the weight of the POM was negligible compared with the weight of the sand, and the mass of this fraction was used for the sand content estimation. Sand correction was carried out according to Six et al. (1998) with the following equation, and the concentration of C stored in aggregates was given in g kg^{-1} bulk soil:

$$\begin{aligned} &\text{C stock}_{\text{size fraction,sand-free}}\left(\text{Mg ha}^{-1}\right) \\ &= \text{C}_{\text{size fraction}}\left(\text{g kg}^{-1}\right) * \left(\text{mass proportion}_{\text{size fraction sand free}}\right) \\ &\quad * \text{dry bulk density}\left(\text{kg dm}^{-3}\right) * \text{depth interval (dm)} \end{aligned} \tag{2}$$

2.5 | Chemical analyses

In addition to samples for aggregation analyses, bulk samples were taken at 0–30-cm, 30–50-cm and 50–70-cm depth horizontal across 1 m of the soil profile wall of the deep-ploughed and reference plots without separation of the buried topsoil and subsoil material in the deep-ploughed plots (see Figure S2). These samples were dried at 40°C in a drying cabinet and sieved at 2 mm.

Bulk soil SOC and N data were used from Alcantára et al. (2016) and were divided in the topsoil (0–30 cm) and subsoil (30–100 cm) to match the data analysis of the other elements. In that study, the reference and deep-ploughed plots were sampled five times.

For the air-dried and sieved bulk soil samples per horizon, aliquots of 5 g were taken and analysed for contents of plant-available phosphate (P_{CAL}) and potassium (K_{CAL}) according to the method of Schüller (1969). After adding the extraction solution, which uses 100 mL buffered solution of 0.05 M Ca-lactate, 0.05 M Ca-acetate and acetic acid, at a pH of 3.7–4.1 and a soil:solution ratio of 1:20 w/v, samples in solution were shaken for 2 h with an overhead shaker and filtered. Then, the concentrations of P_{CAL} were determined photometrically with the molybdenum-blue-coloration method (Murphy & Riley, 1962) on a Specord 205 photometer (Analytik Jena AG, Germany). K_{CAL} concentrations were measured by atomic absorption spectroscopy (AAS, A Analyst 300, PerkinElmer).

Air-dried and sieved bulk soil samples to 50-cm depth were homogenized with a vibratory disk mill (tungsten carbide grinding set) and pressed into pellets and analysed as fused discs for their total P, K, aluminium (Al), and iron (Fe) oxide concentrations by a wavelength dispersive X-ray fluorescence (XRF) spectrometer (Axios, 3 kW, PANanalytical GmbH). The specific oxide counts were normalized for the loss on ignition (LOI) of organic matter by heating to 1100°C for 2 h (Kehl et al., 2014; Vlaminck et al., 2018).

2.6 | Data analysis

Statistical analyses were carried out in R (version 4.2.0) (R Core Team, 2022), using the packages ggplot2, RColorBrewer, tidyverse, broom, sf, dplyr, lme4, lmerTest, rstatix and agricolae.

Pearson correlations were calculated for root biomass and bulk density in the subsoil, as well as the amount of buried topsoil and root biomass in the subsoil and between the bulk density and amount of buried topsoil in the subsoil. The variables bulk density and root biomass were detrended for the depth in cm in order to correct for the influence of depth in these variables, which allows us to analyse other trends in soil properties throughout the whole soil profile than the influence of soil depth, since it has high explanatory power.

The SOC and N stocks for the total profile were already assessed by Alcantára et al. (2017, 2016); in order to see the effects on the topsoil and subsoil separately, these data were used to calculate the SOC and N stocks for the depth intervals 0–30 cm and 30–100 cm. A Pearson correlation was carried out between the SOC and N stocks to analyse the effects of deep-ploughing on the two parameters. After that, this data was compared to the C concentrations and C stock to estimate the SOC stock associated to aggregates. The topsoil and subsoil SOC, N, P_{CAL} and K_{CAL} stocks, as well as root biomass at different depths and the bulk densities at 0–30-cm depth and aggregates at 0–30-cm and 50–70-cm depth interval in the deep-ploughed plots were compared with the respective controls by performing linear mixed-effects models (normal distribution of data was confirmed). The sites were used as the random effects and random intercepts and slopes were incorporated in the model to allow treating the three soil profiles as pseudo replicates with potential spatial dependencies, despite profiles being located 30–80 m apart from another. Significant differences between means were then further explored by pairwise *t*-tests with Bonferroni correction as post hoc tests.

Since the data on SOC and N stocks were derived from Alcantára et al. (2016) and each treatment was sampled five times, five pseudo replicates were used. As the root biomass and soil moisture were sampled per horizon, which differed per field, linear mixed models were

used in the same way as described before, but depth was used as a nested random effect within the site. Significant differences between means were then further explored by pairwise *t*-tests with Bonferroni correction as post hoc tests as well. Differences were assigned as significant for a $p < 0.05$ level of probability, and as almost statistically significant for $0.05 < p < 0.1$. Bulk density and aggregate samples in the subsoil were additionally separated into the former topsoil and turned B horizon, we added this horizon as a nested effect in the linear mixed-effects model and compared the differences per depth class and horizon with descriptive statistics.

The choice for using pseudo replicates is not ideal, since type I errors might be produced and caution should be taken interpreting these results (Webster & Lark, 2019). However, it is justifiable considering the value and uniqueness of these on-farm trials with an age of over 50 years (Davies & Gray, 2015). Yet, it has to be kept in mind that all analyses is thus specific for the given site and management conditions, that is, extrapolations to other geographical or environmental settings have to be considered with care.

3 | RESULTS

3.1 | Yield

At all the three sites, the deep-ploughed plots showed higher above-ground productivity at the time of sampling in 2019 than the control plots, as evident for grain yield and straw yield (Table 2). The grain yield on the deep-ploughed plots was 6%–57% higher than that at the reference plots for Banteln, Elze, and Essemühle, respectively. The straw yield at the deep-ploughed plots exceeded that of the reference plots by 9%–43%. The higher grain and straw yield were only significant in Essemühle ($p < 0.05$ and $p < 0.05$). A positive effect was also observed for the thousand grain weight and the number of ears. The thousand grain weight at the deep-ploughed plots was 15% and 11% higher for Banteln ($p < 0.05$) and Essemühle, respectively, but similar on the deep-ploughed plots in Elze when compared with the reference plots. The number of ears for the deep-ploughed plots were 0.4%–17% higher than for the reference sites at Banteln, Elze, and Essemühle respectively, but this was not significant.

TABLE 2 Yield parameters for the three sites (Banteln, silt loam; Elze and Essemühle, loamy sand) per treatment in 2019 and 2020.

Site	Year	Treatment	Grain yield[a] (t ha^{-1})	Straw yield (t ha^{-1})	Thousand grain weight (g)	Number of ears per m^2
Banteln	2019	Reference	5.8 (0.32). *12.1*	6.4 (0.35) *12.2*	35.1 (1.5) * *9.4*	440 (19) *9.6*
		Deep-ploughed	7.4 (0.65) *19.6*	7.0 (0.62) *19.7*	40.3 (1.1) * *6.2*	506 (55) *24.2*
	2020	Reference	6.1 (0.57) *20.7*	6.9 (0.70) *22.8*	40.2 (0.7) *3.6*	531 (43) *18.2*
		Deep-ploughed	6.6 (0.32) *10.8*	6.8 (0.39) *12.6*	40.6 (0.4) *2.2*	515 (13) *5.6*
Elze	2019	Reference	6.2 (0.20) *7.0*	8.0 (0.25) *7.0*	30.3 (0.4) *3.2*	398 (16) *8.9*
		Deep-ploughed	6.6 (0.56) *19.1*	8.7 (0.28) *7.2*	30.0 (0.8) *6.2*	399 (99) *55.7*
	2020	Reference	-	-	-	-
		Deep-ploughed	-	-	-	-
Essemühle	2019	Reference	4.0 (0.17) * *9.3*	5.6 (0.23) * *9.2*	24.8 (0.9) *8.2*	383 (14) *8.5*
		Deep-ploughed	6.4 (0.38) * *13.2*	8.0 (0.56) * *15.6*	27.4 (1.4) *11.5*	446 (20) *9.9*
	2020	Reference	4.0 (0.47) *** *26.2*	3.2 (0.38) * *27.3*	31.3 (2.2) *15.7*	321 (35) *24.7*
		Deep-ploughed	6.5 (0.21) *** *7.2*	4.6 (0.38) * *18.7*	36.2 (0.6) *3.6*	349 (17) *24.7*

Note: SEM is written in parentheses ($n = 5$) and relative SD is written in italic. Significant differences are displayed by '.', '*', '**', or '***', indicating a *p*-value of lower than 0.1, 0.05, 0.01, or 0.001.

[a]Winter wheat in Banteln and winter rye in Elze and Essemühle, no data from Elze in 2020 since no cereal crops were grown on the field.

It should be noted that SDs for grain yield, straw yield and stand density were generally higher for deep-ploughed plots at all sites of investigation. In 2020, yield effects were similar in Essemühle as in 2019 with significantly higher grain yield ($p < 0.001$) and straw yield ($p < 0.05$) at the deep-ploughed plot. In Banteln, there were no significant differences between the deep-ploughed and reference plot in 2020, but yield parameters except from the grain yield and thousand grain weight were lower in Banteln (Table 2).

The yield assessment in the field did not reflect farmers' impressions over the years (particularly for Banteln they reported on negative impacts of deep-ploughing on yields; in Essemühle, in turn, they were positive); hence, yields were crosschecked using satellite data. The analyses showed that multiannual NDVI values (Table S1) between April and June were significantly lower for the deep-ploughed part of the field in Banteln than for the reference plot ($p < 0.05$) and between 2016 and 2022, the NDVI values were lower every year in the deep-ploughed plots than the reference plots, except for the year 2021 (Figures S3 and S4). In Elze and Essemühle, multiannual NDVI values between April and June were significantly higher in the deep-ploughed plot than in the reference one ($p < 0.05$). In Elze, they were higher in the deep-ploughed pots every year, but only in 2018, 2019 and 2020 in the deep-ploughed plots in Essemühle. Lower NDVI values in the deep-ploughed plots can indicate lower yields than at the non-deep-plouhged plots, whereas higher NDVI values indicate higher yields.

3.2 | Root biomass and bulk density

Deep-ploughing has been designed to facilitate subsoil access by roots. Overall, root biomass (in mg per cm^3 soil) was significantly higher at one sandy site ($p < 0.01$, Essemühle) and significantly lower ($p < 0.05$) at the other sandy site (Elze). At the silty site, the root biomass tended to be lower, but this was not significant (Figure 2). In the subsoil in Banteln, the root biomass was generally lower in the deep-ploughed plots than in the adjacent silty reference plots, with the largest difference occurring at 70–90 cm depth ($p < 0.05$). In Essemühle, the root biomass was significantly elevated in the deep-ploughed plots compared with reference plots ($p < 0.05$), with large differences at 40–50 cm depth ($p < 0.01$), at 50–60 ($p < 0.01$) and at 60–70 cm depth ($p < 0.05$). There were no significant differences in root biomass in the different horizons in Elze. Hence, and unlike yield development in the year of sampling, the response of current root biomass to former deep-ploughing was mostly site-specific.

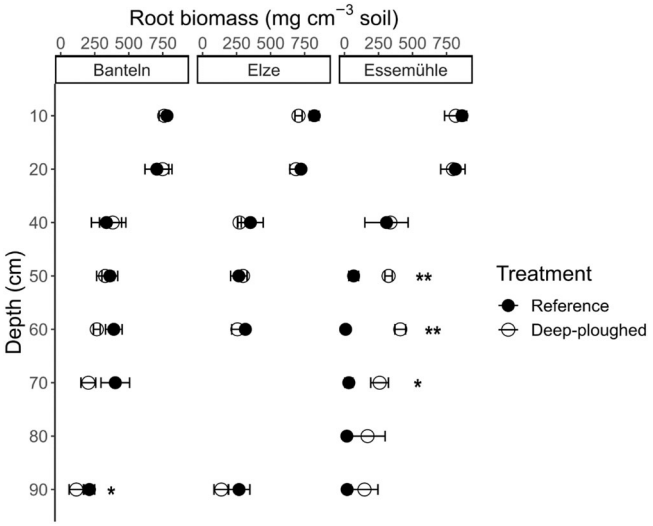

FIGURE 2 Root biomass of the reference plot and the deep-ploughed plots per site. The crops grown were winter wheat in Banteln and winter rye in Elze and Essemühle. Error bars represent the SEM ($n = 3$). Significant differences are displayed by '.' $p < 0.1$, '*' $p < 0.05$, '**' $p < 0.01$ and '***' $p < 0.001$.

Apart from the breaking of root-restricting layers, another aspiration of deep-ploughing has been the lowering of bulk density in the subsoil (Schneider et al., 2017). The average bulk densities of Banteln, Elze and Essemühle in the topsoil were 1.22, 1.46 and 1.37 g cm^{-3} respectively, while those of the subsoil ranged between 1.50 g cm^{-3} for Banteln and 1.52 g cm^{-3} for Elze and Essemühle, respectively. The bulk densities for the specific treatments and horizons are displayed in Figure 3. The change in bulk density after deep-ploughing was site-specific. At the silty site Banteln, bulk densities in the first 50 cm had significantly increased after deep-ploughing: in the topsoil, bulk density was increased by 0.1 and 0.11 g cm^{-3} at 10 and 20-cm depths respectively, whereas deep-ploughing increased the bulk density by 0.6 and 0.8 g cm^{-3} in the buried topsoil and B horizon compared with the reference plot (Figure 3). Bulk densities in Essemühle were reduced at 45 cm depth in the buried topsoil compared with the refence soils (by 0.12 g cm^{-3}) and by 0.14 g cm^{-3} at 65 cm depth. In Elze, bulk densities were reduced by 0.11 and 0.06 g cm^{-3} at 50-cm depth in the buried topsoil and B horizon of the deep-ploughed plot respectively, compared with the reference plot.

Changes in bulk densities >50 years after deep-ploughing were opposite to the trends for roots. Table 3 and Figure S5 show the correlation coefficients between root biomass, bulk density and the amount of buried topsoil in the sample, detrended for different depth intervals (cm). Indeed, bulk density was negatively correlated with

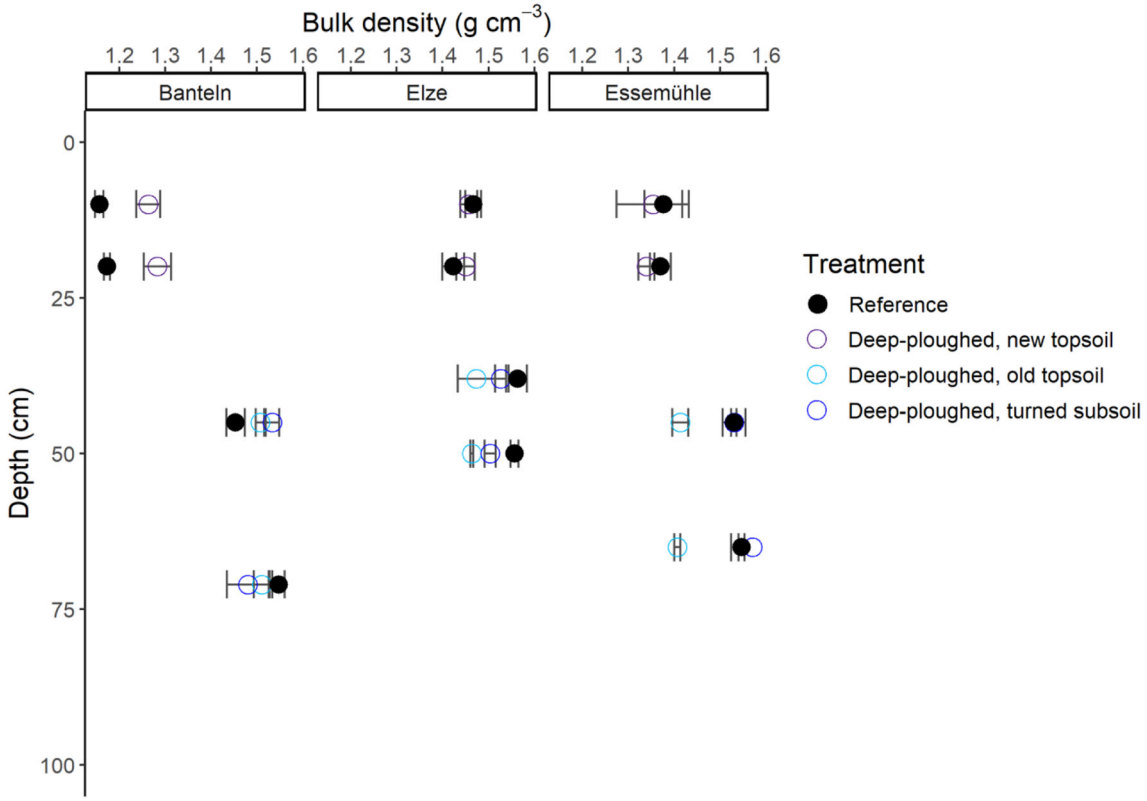

FIGURE 3 Average bulk density of the reference plot and the deep-ploughed plots per site. Error bars represent the SEM (reference plots $n = 3$).

TABLE 3 Pearson correlation coefficients of root biomass, bulk density and the amount of buried topsoil in the sample in the subsoil (30–100 cm) and upper subsoil (30–50 cm) detrended for depth (cm) and excluding the topsoil (<30 cm).

Site	Bulk density		Amount of buried topsoil in sample	
Correlation with root biomass		Upper subsoil		Upper subsoil
Banteln	−0.05	0.07	0.03	0.03
Elze	−0.23*	−0.10	0.17.	0.06
Essemühle	−0.58***	−0.55***	0.51***	0.45**
Correlation with bulk density				Upper subsoil
Banteln			0.14	0.52***
Elze			−0.56***	−0.48***
Essemühle			−0.86***	−0.82***

Note: Significant correlations are indicated by '.' ($p < 0.1$) '*' ($p < 0.05$), '**' ($p < 0.01$), or '***' ($p < 0.001$).

the amount of root biomass, though not in similar manner for all three sites. In Banteln, the silty site, the correlations were not significant (Table 3, Figure S5A). Bulk density and root biomass were negatively and significantly correlated in Elze ($p < 0.05$) and Essemühle ($p < 0.001$). Also, the amount of buried topsoil in the sample (Table S2, Figure S5) correlated positively with root biomass, particularly for site Essemühle, and thus negatively with bulk density. The correlations were again not significant for the silty site Banteln, except for the correlation between the buried topsoil and bulk density in the upper subsoil (30–50 cm), which was positive (0.5, $p < 0.001$). In Elze, the correlation between bulk density and the buried topsoil was stronger in the upper subsoil (−0.72, $p < 0.001$) than in the total subsoil (Table 3, Figure S5B).

3.3 | Sand-free aggregates

Sand-free aggregates accounted for 75%, 12%, and 10% of soil mass in Banteln, Elze, and Essemühle, respectively (Figure S6). This was more than those in the adjacent deep-ploughed plots, but this difference was the largest

in Elze, where the amount of aggregates per kg soil decreased by 29% after deep-ploughing.

Persistence of improved subsoil conditions is frequently associated with improved aggregation. In the subsoil, at 30–50-cm depth, the sand-free aggregates accounted for 57% of the dry soil mass in the reference plots of Banteln, 12% in Elze, and 10% in Essemühle, respectively. Particularly in the buried topsoil stripes, aggregation differed: it had increased in Banteln, but it had declined in Elze (decrease of 49%) and Essemühle, respectively. A similar trend was observed at 70 cm soil depth: a higher level of aggregation in the buried topsoil relative to the original subsoil at the silty site Banteln and no change at the sandy sites (Figure 4). Compared with the topsoil of the control plots, the buried topsoils contained less aggregates at 50-cm depth in Banteln (7.7% less) and Elze (46% decrease) but did not show any differences in Essemühle. At 70-cm depth, the amount of aggregates was not significantly different from the topsoil of the control plot at all sites. Hence, the effects were again site- and depth-specific.

With changes in total amounts of sand-free aggregates, their size distribution also changed. At all the sites, less large macroaggregate fraction (>2000 μm) was found in the topsoil of the deep-ploughed plots compared with the adjacent reference plots, but the linear mixed model was not significant. In Banteln and Elze, this was approximately 40% and 51% less, respectively. The small macroaggregate fraction (2000–250 μm) also exhibited lower contents in the deep-ploughed plot in Banteln, since it was not present in the deep-ploughed plot. In the buried topsoil parts of the subsoil, the portions of the different aggregate fractions did not show uniform effects across the three sites. The amount of small microaggregates (<53 μm) was 75% larger after former deep-ploughing at the silty site Banteln at 30–50-cm depth. Larger microaggregates were more abundant as well, but smaller macroaggregates were less, although these changes were small.

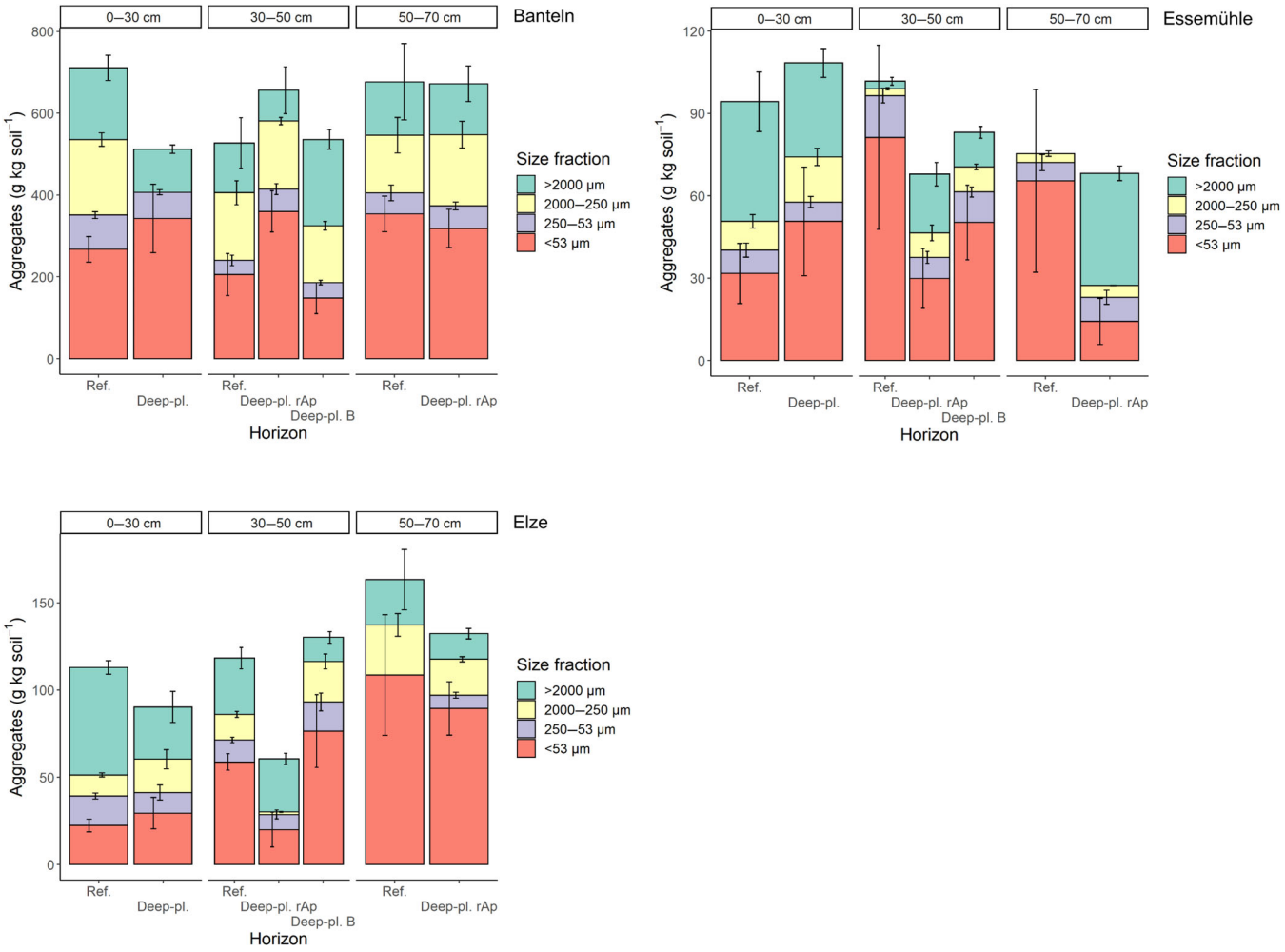

FIGURE 4 Mass of sand-free aggregates in g kg^{-1} soil in different size fractions in the reference plot and deep-ploughed plot in Banteln, Elze, and Essemühle. The measurements are taken from 0 to 30 cm depth, 30 to 50 cm depth (in the deep-ploughed plots), and 50 to 70 cm. Error bars represent the SEM ($n = 3$).

At the sandy sites in turn, the small microaggregates occurred in lower proportions at 50-cm depth, that is, aggregate size increased, on average, and showed a 60% loss, but with relatively large SE in Elze. The proportions of the small and large macroaggregates (250–2000 μm, >2000 μm) changed in opposite direction: there were little if any changes in the surface soils and in the silty subsoil at Banteln and sandy subsoil of Elze, but the proportion of large aggregates increased at the expense of the smaller aggregate fractions in the subsoil of Essemühle. This latter effect was almost significant for the small aggregates at 50 cm depth due to large SE and visible for the larger aggregates at this depth (increase of 600%) and for large macroaggregates at 70-cm depth (from no large macroaggregates to 40.9 g kg^{-1} soil).

3.4 | Element contents

SOC stocks within the whole soil profile were, on average, 14% and 26% larger in the deep-ploughed plots than their respective reference counterparts (Figure 5a: Alcantára et al. (2016)); the N stocks were 6%–48% larger (Figure 5b). This gain in SOC stock was significant for

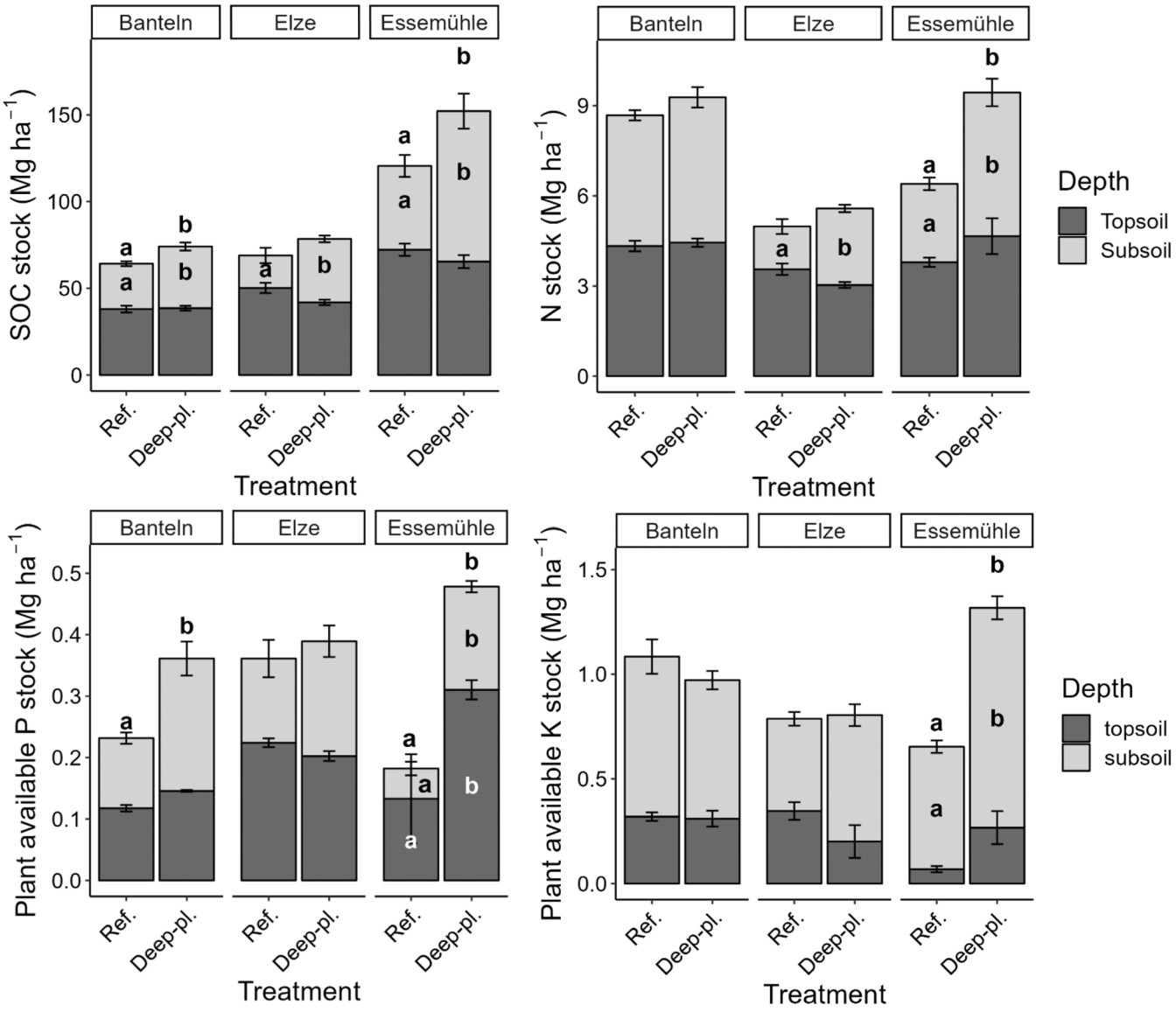

FIGURE 5 Topsoil (0–30 cm) and subsoil (30–100 cm) nutrient stocks per site, including the adjacent reference plot and the deep-ploughed plot for the following nutrients: (a) SOC, (b) N, (c) plant-available P (P_{CAL}), (d) plant-available K (K_{CAL}). The error bars represent the SEM (soil organic carbon [SOC] and N stocks: $n = 5$, plant-available P and K: $n = 3$). Different letters indicate statistical differences ($p < 0.05$) between reference and deep-ploughed plots for a given horizon per site. For SOC and N stocks, data from Alcantára et al. (2016) were reanalysed.

Banteln ($p < 0.05$) and visible in Essemühle ($p < 0.05$); N stocks were significantly elevated in Essemühle only ($p < 0.01$). Overall, 50 years after deep-ploughing, the gain in SOC was due to significant SOC accrual in the uplifted subsoil, which was more than the loss from the buried subsoil of all the three sites ($p < 0.05$), except from Elze where SOC was lost from both depth increments ($p < 0.1$). Changes in total N stocks followed those of SOC stocks ($r = 0.87$; $p < 0.001$).

In Banteln, 90% of topsoil SOC in the reference plots was stored in aggregates, but only 46% in the deep-ploughed plot (Figure S7A). This effect was similar at the sandy sites, where 23% and 19% of SOC was stored in aggregates at the reference plots of Elze (Figure S7B) and Essemühle (Figure S7C), respectively, while 15% and 12% of SOC were stored in the aggregates of the respective deep-ploughed plots. In the subsoil, the effect of deep-ploughing was different. In the subsoil of Banteln, 55% and 72% of the SOC stock was stored in aggregates in the reference plot and deep-ploughed plot, respectively. At the sandy sites, the percentage of the SOC stock stored in aggregates was similar in the deep-ploughed subsoil and reference subsoil, with 23% and 10% in Elze and Essemühle, respectively.

The aggregate-SOC stock was lower in the topsoils of the deep-ploughed plots than in the reference ones, but this was not significant in the linear mixed-effects model (Figure S7). In the subsoil, this trend was reversed: aggregate-SOC stocks were elevated in the buried topsoils stripes compared with the subsoils of the reference sites, except in Elze, where aggregate-SOC stocks were lower by 49%. When comparing the buried topsoils in the deep-ploughed soils with the topsoils of the reference plots, the aggregate-SOC stock was 72% lower in the buried topsoil in Banteln, 76% lower in the buried topsoil in Elze, and 85% lower in that of Essemühle, all compared with the topsoil of the reference plot.

Most of the aggregate-SOC stock in the buried topsoils was lost from macroaggregates, when they were compared with the topsoils (0–30 cm) of the reference plots. In Banteln, the large macroaggregates (>2000 μm) showed largest decrease in aggregate-SOC stock, a loss of 88% and 82% at 50 and 70-cm depths in the buried topsoil respectively compared to the topsoil (0–30 cm depth) of the reference plot. In Elze, the smaller macroaggregates (2000–250 μm) lost the most aggregate-SOC, accounting for a 97% decrease in the buried topsoil at 50 cm depth. In Essemühle, again large macroaggregates lost most of the aggregate-SOC stock at 50 cm depth (85%), whereas most aggregate-SOC was lost from smaller macroaggregates at 70 cm depth (86%).

At all sites, the plant-available phosphorus (P_{CAL}) stocks had increased in the subsoil and partly even in the topsoil after deep-ploughing, which was significant for Banteln ($p < 0.05$) and Essemühle ($p < 0.01$) (Figure 5c). The gain in available P after former deep-ploughing was smaller in the topsoil (12%–23%) than in the subsoil (34%–147%; Figure 5c). Plant-available P accounted for approximately 6% of total P in both top- and subsoil at the deep-ploughed plots in Banteln, while this contribution was 9%–13% to total P in the sandy topsoils, and 22%–29% in the subsoils of Elze and Essemühle (for total P and K stocks, see Table S3; Supplementary material).

Unlike P, changes in the stocks of plant-available potassium (K_{CAL}) were ambiguous. The K_{CAL} stocks within the soil profile decreased in the silty soil of Banteln in the topsoil and subsoil, remained more or less unchanged at the sandy site Elze due to a decrease in the topsoil and an increase in the subsoil, but increased by 288% and 91% in the top- and subsoil of Essemühle, respectively, which was significant in the subsoil ($p < 0.01$). The increase of total plant-available K stocks in Essemühle was significant ($p < 0.01$). Hence, changes in the soil K_{CAL} pool from former deep-ploughing were clearly site-specific (Figure 5d).

4 | DISCUSSION

4.1 | Yield, roots and changes in physical soil properties

Deep-ploughing in Northern Germany lost popularity in the 1970s and was not expanded to a larger area, because its long-term effects on the yield were inconsistent (Foerster, 1974; Grosse, 1974; Scheffer & Meyer, 1970). The deep-ploughed loamy and silty soils showed a loosening effect only for 1 year after deep-ploughing, but they were more compacted afterwards (Hartge, 1980). Also, the current farmers at our field sites, except from Essemühle, were obviously not fully convinced of this former intervention, as they did not only deep-plough the whole fields but only parts of it. Indeed, yields were eventually reduced in some years, especially at Banteln.

The subsoil also stores a significant part of plant-available water (Schneider & Don, 2019a, 2019b). Hence, breaking root-restricting layers may be beneficial for yields particularly in dry years (Gaiser et al., 2013; Schneider et al., 2017; Sun et al., 2018). Indeed, in the relatively dry years 2019 and 2020, almost all yield components of the deep-ploughed plots outperformed those of the reference plots at the sandy sites. At the silty site, the effects were less consistent; in 2019, the yield of the deep-ploughed plot was higher, but in 2020, this was only the case for grain yield and the weight of a thousand grains. Q. Feng et al. (2020) found that deep tillage changed grain yield by between −3% and 23%, on average, but

had negative effects mostly at loamy and silty sites, which is in line with results reported by Schneider et al. (2017).

The multi-year NDVI data (Table S1 and Figures S3 and S4) confirmed the positive effects at the two sandy sites, but indicated negative effects of deep-ploughing on yields in silty Banteln. This suggests that in general the effects of deep-ploughing on total above-ground biomass were negative but that due to patchiness and heterogeneity, certain specific yield parameters such as weight of a thousand grains can still show positive effects of deep-ploughing. It should also be noted that the biomass sampling was carried out in July, when the NDVI values of the deep-ploughed plots were slightly higher than those of the reference plots in Banteln, but the average NDVI difference between the deep-ploughed plot and reference plot was negative between April and June in 2016–2022. Yet, our analyses show that crosschecking yields via satellite data may generally be needed for long-term assessments of management effects on soil performance.

Intriguingly, yield gain was only partly supported by enhanced root growth in the deep-ploughed subsoil, with clear effects for Essemühle only. At this site, increased root biomass showed the strongest relationship to reductions in bulk density (Table 3), while at the other sites other factors than total root biomass likely contributed to changes in yield (Table 2, Figure 2). One of these factors might be soil moisture (Table S4; Rossato et al. (2017)), which was slightly lower in Banteln subsoil (70–85 cm, $p < 0.05$) but higher in Essemühle ($p < 0.01$ at 0–30 cm depth, $p < 0.05$ at 70–75 cm depth). Another factor might be the drought tolerance of the crop selected: winter rye grew at the sandy sites. It is usually more drought-tolerant than winter wheat (Schittenhelm et al., 2014), which was grown in Banteln.

Han et al. (2022) analysed biopores at the sites Banteln and Elze. The authors found only few biopores in both deep-ploughed and reference plots in sandy Elze. In Banteln, biopores were more abundant, though significantly less in the deep-ploughed plots than in the reference ones. As biopore formation supports deep root development (Kautz et al., 2013; Wendel et al., 2022), this disruption of biopore density likely additionally hampered optimum yield development at Banteln.

A final factor that likely contributed to yield development is soil structure. At Essemühle, the buried topsoil stripes contained more macroaggregates than the reference plots, thus facilitating water infiltration and deep root growth even 50 years after deep-ploughing (Figure 2). The incorporation of organic matter, in turn, could stabilize the aggregates and promote new aggregate formation. As macroaggregates are mainly held together by fine roots (Jastrow et al., 1996; Six et al., 2000; Waters & Oades, 1991), the improved subsoil rooting as well as higher overall yields correlated with the higher degree of macroaggregation. Likely, at this sandy site, a positive feedback loop developed: the loosened subsoil, a long-term effect of deep-ploughing, facilitated the growth of deep-rooting systems, which then stabilized soil aggregates as macroaggregates and therewith lowered bulk density and again promoted subsoil rooting. The effects at Elze were intermediate, likely due to its shallower deep-ploughing depth (Cai et al., 2014). At the silty site Banteln, in turn, the portion of macroaggregates in the subsoil had declined and microaggregates dominated, reflecting the breakdown of macroaggregates into their microaggregate building units indicating soil compaction as well (Elliott, 1986; Six et al., 2000; Tisdall & Oades, 1982). In general, silty soils with degraded soil structure and low clay, colloid and SOC content are more prone to soil compaction and recover slower by cultivation than coarser textured soils (Horn et al., 1995; Nawaz et al., 2013). This can lead to a further breakdown of soil structure and impaired root growth into soils due to increased mechanical penetration resistance that impairs yields (Lipiec & Simota, 1994; Pöhlitz et al., 2020).

Since this study uses pseudo-replicates due to a lack of true replication, the analyses of soil physical properties and their extrapolation to different soil types in different climates should be done with caution as the results of deep-ploughing are site-specific. However, many other studies have reported similar results on soils with deep tillage, which also support our results (Alcantára et al., 2016, 2017; Botta et al., 2006; Cai et al., 2014; Han et al., 2022).

4.2 | Element contents

The SOC and N stocks were larger in the deep-ploughed than in the reference plots at all three sites (Alcantára et al., 2016). This gain in SOC and total N stocks was largest in the subsoils (30–100 cm), due to the burial of SOM (Morari et al., 2019) and SOM accrual in the newly formed topsoil (X. Feng et al., 2018). However, in Elze, topsoil C and N stocks in the deep-ploughed plots were still reduced compared with the reference plots, thus maintaining a legacy of the mixing of the former subsoil with the former topsoil, which can be compensated by (organic) fertilization (Alcantára et al., 2016). Our findings are again in line with those of Q. Feng et al. (2020), who also found that topsoil SOC stocks can initially decrease after deep-ploughing due to mixing with the SOC poor subsoil. The rates at which the SOC stocks in the newly formed topsoil recover depend on several factors such as texture, (organic) fertilization and ploughing

of the topsoil (Alcantára et al., 2016; Baer et al., 2010; Morari et al., 2019). Also own recent findings indicate that particularly in sandy soils a complete recovery of degraded sandy topsoil is possible within a few decades at good agricultural management practice, as well as the preservation of buried topsoil material under the right fertilization regime (Burger et al., 2023). Altogether, deep-ploughing thus frequently causes a net increase in SOC stocks of the total profile (Alcantára et al., 2016), which persisted here even after 50 years.

In Banteln and Essemühle, where the SOC stock was higher in the buried topsoils than in the reference subsoils, a larger part of the subsoil SOC stock was stored within aggregates after deep-ploughing. Similar observations were made by Plaza-Bonilla et al. (2010), who found for loamy soils in Spain that reduced tillage improved the aggregate formation and C sequestration in the first 5 cm of the profile, but that conventional ploughing, with mouldboard ploughing until 40 cm stored more SOC in below 20 cm depth, despite having a similar amount of macroaggregates at this depth. Alcantára et al. (2017) found that subsoil SOC was less easily decomposed than that of the topsoils, which is generally the case when exposed to labile C sources and formerly limiting nutrients (Fontaine et al., 2007; Meyer et al., 2018).

With the accrual of SOM, other nutrients also usually accumulate, such as plant-available P (P_{CAL}), most prominent in the subsoil and in Essemühle. An increase in total P and plant-available P was also found by Cai et al. (2014) and Sharpley (2003) after deep-ploughing due to mixing of P rich topsoil with P poorer subsoil; hence, the topsoil may thus require additional P fertilization (Cai et al., 2014; Holanda et al., 1998; Sharpley, 2003).

While available P can also be released by the mineralization of SOM, plant-available potassium (K_{CAL}) is usually only released from mineral surfaces. Deep-ploughing influenced plant-available K in the same way as it did plant-available P, that is, redistributing K from K rich topsoil into the subsoil (Holanda et al., 1998; Sharpley, 2003). Lower plant-available K stocks in the topsoil of the deep-ploughed plots in Banteln and Elze reflected that the topsoil material was diluted with material poorer in K from the subsoil. Only in Essemühle dilution of available K by deep-ploughing and plant uptake was likely compensated by fertilization. At all the sites, the soil mixing had increased the stocks of plant-available K in the subsoil (Holanda et al., 1998; Sharpley, 2003), which here was still detectable after 50 years.

Additionally, plant-available P and K stocks could be positively influenced by the reduction of pH in the subsoil (supplemental material of Alcantára et al. (2016)) and preservation of soil moisture (Holanda et al., 1998; Riekerk, 1971; Zeng & Brown, 2000). Cai et al. (2014), for instance, found that deep-ploughing improved soil moisture status during growing periods. However, we cannot conclusively assign our results to these effects, as soil moisture could only be determined at the day of sampling but not as integral over the whole vegetation period.

5 | CONCLUSION

Our study revealed a legacy of deep-ploughing on crop performance, that was still detectable 50 years after soil intervention. At the sandy sites, we observed improved yields in the deep-ploughed plots, particularly at the dry hot summer of the sampling year, which was related to reduced bulk density, increased macroaggregation and incorporation in the buried topsoil stripes, and thus increased root growth. At the silty site, a more uniform distribution of macronutrients within the soil profile was observed as well, but no clear positive effects of deep-ploughing on soil structure, root biomass and yield. Hence, both direction and degree of such legacy effects of former deep-ploughing were site-specific, likely controlled by texture and furthermore altered by fertilization and possibly depth of former deep-ploughing. Overall, deep-ploughing is thus not recommended on silty soils derived from loess, but could be an opportunity on sandy soils.

AUTHOR CONTRIBUTIONS

Dymphie J. Burger: Writing – original draft; investigation; formal analysis; data curation; visualization. **Florian Schneider:** Writing – review and editing; investigation; data curation; formal analysis; software. **Sara L Bauke:** Writing – review and editing; supervision; project administration; investigation; methodology; conceptualization; validation. **Timo Kautz:** Writing – review and editing; funding acquisition; supervision; project administration; conceptualization. **Axel Don:** Writing – review and editing; funding acquisition; validation; supervision; project administration; conceptualization. **Wulf Amelung:** Writing – review and editing; funding acquisition; supervision; project administration; validation; conceptualization.

ACKNOWLEDGEMENTS

We thank F. Hegewald (Thünen), K. Unger and A. Lindecke (Bonn) for help during sampling and basic soil analyses and Sven-Oliver Franz for XRF analyses. Funding is acknowledged from the German Federal Ministry of Education and Research (BMBF) in the framework of the funding measure 'Soil as a Sustainable Resource for the Bioeconomy – BonaRes', project BonaRes (Module A): BonaRes Center for Soil Research, subproject 'Sustainable Subsoil Management – Soil[3]'

(grants 031B0151A, 031B0151E and 031B0151G). Open Access funding enabled and organized by Projekt DEAL.

DATA AVAILABILITY STATEMENT

The data that support the findings of this study are available from the corresponding author upon reasonable request.

ORCID

Dymphie J. Burger https://orcid.org/0000-0002-8773-3578
Florian Schneider https://orcid.org/0000-0003-3036-6284
Sara L. Bauke https://orcid.org/0000-0003-2284-9593
Axel Don https://orcid.org/0000-0001-7046-3332

REFERENCES

Alcantára, V., Don, A., Vesterdal, L., Well, R., & Nieder, R. (2017). Stability of buried carbon in deep ploughed forest and cropland soils – implications for carbon stocks. *Scientific Reports*, *7*(5511), 1–12. https://doi.org/10.1038/s41598-017-05501-y

Alcantára, V., Don, A., Well, R., & Nieder, R. (2016). Deep ploughing increases agricultural soil organic matter stocks. *Global Change Biology*, *22*(2939–2956), 2939–2956. https://doi.org/10.1111/gcb.13289

Amtmann, A., & Blatt, M. R. (2009). Regulation of macronutrient transport. *The New Phytologist*, *181*(1), 35–52. https://doi.org/10.1111/j.1469-8137.2008.02666.x

Baer, S. G., Meyer, C. K., Bach, E. M., Klopf, R. P., & Six, J. (2010). Contrasting ecosystem recovery on two soil textures: Implications for carbon mitigation and grassland conservation. *Ecosphere*, *1*(1), 1–22. https://doi.org/10.1890/ES10-00004.1

Beck-Broichsitter, S., Gerke, H. H., Leue, M., von Jeetze, P. J., & Horn, R. (2020). Anisotropy of unsaturated soil hydraulic properties of eroded Luvisol after conversion to hayfield comparing alfalfa and grass plots. *Soil and Tillage Research*, *198*, 104553. https://doi.org/10.1016/j.still.2019.104553

Berisso, F. E., Schjønning, P., Keller, T., Lamandé, M., Simojoki, A., Iversen, B. V., Alakukku, L., & Forkman, J. (2013). Gas transport and subsoil pore characteristics: Anisotropy and long-term effects of compaction. *Geoderma*, *195–196*, 184–191. https://doi.org/10.1016/j.geoderma.2012.12.002

Botta, G. F., Jorajuria, D., Balbuena, R., Ressia, M., Ferrero, C., Rosatto, H., & Tourn, M. (2006). Deep tillage and traffic effects on subsoil compaction and sunflower (*Helianthus annus* L.) yields. *Soil and Tillage Research*, *91*(1–2), 164–172. https://doi.org/10.1016/j.still.2005.12.011

Burger, D. J., Bauke, S. L., Amelung, W., & Sommer, M. (2023). Fast agricultural topsoil re-formation after complete topsoil loss – Evidence from a unique historical field experiment. *Geoderma*, *434*, 116492. https://doi.org/10.1016/j.geoderma.2023.116492

Cai, H., Ma, W., Zhang, X., Ping, J., Yan, X., Liu, J., Yan, J., Wang, L., & Ren, J. (2014). Effect of subsoil tillage depth on nutrient accumulation, root distribution, and grain yield in spring maize. *The Crop Journal*, *2*, 297–397. https://doi.org/10.1016/j.cj.2014.04.006

Davies, G. M., & Gray, A. (2015). Don't let spurious accusations of pseudoreplication limit our ability to learn from natural experiments (and other messy kinds of ecological monitoring). *Ecology and Evolution*, *5*(22), 5295–5304. https://doi.org/10.1002/ece3.1782

do Rosário, M., Oliveira, G., van Noordwijk, M., Gaze, S. R., Brouwer, G., Bona, S., Mosca, G., & Hairiah, K. (2000). Auger sampling, ingrowth cores and pinboard methods. In A. L. Smit, A. G. Bengough, C. Engels, M. van Noordwijk, S. Pellerin, & S. C. van de Geijn (Eds.), *Root methods: A handbook* (pp. 174–210). Springer. https://doi.org/10.1007/978-3-662-04188-8_6

Durgun, Y. Ö., Gobin, A., Duveiller, G., & Tychon, B. (2020). A study on trade-offs between spatial resolution and temporal sampling density for wheat yield estimation using both thermal and calendar time. *International Journal of Applied Earth Observation and Geoinformation*, *86*, 101988. https://doi.org/10.1016/j.jag.2019.101988

Elliott, E. T. (1991). Organic matter contained in soil aggregates from a tropical chronosequence: Correction for sand and light fraction. *Agriculture, Ecosystems and Environment*, *34*, 443–451. https://doi.org/10.1016/0167-8809(91)90127-J

Elliott, E. T. (1986). Aggregate structure and carbon, nitrogen, and phosphorus in native and cultivated soils. *Soil Science Society of America Journal*, *50*(3), 627–633. https://doi.org/10.2136/sssaj1986.03615995005000030017x

Feng, Q., An, C., Chen, Z., & Wang, Z. (2020). Can deep tillage enhance carbon sequestration in soils? A meta-analysis towards GHG mitigation and sustainable agricultural management. *Renewable and Sustainable Energy Reviews*, *133*, 110293. https://doi.org/10.1016/j.rser.2020.110293

Feng, X., Hao, Y., Latifmanesh, H., Lal, R., Cao, T., Guo, J., Deng, A., Song, Z., & Zhang, W. (2018). Effects of subsoiling tillage on soil properties, maize root distribution, and grain yield on mollisols of northeastern China. *Agronomy Journal*, *110*(4), 1607–1615. https://doi.org/10.2134/agronj2018.01.0027

Foerster, P. (1974). Ergebnisse des Tiefpflügens in Sandböden Norddeutschlands. *Landbauforschung Volkenröde: Sonderheft*, *24*, 47–67.

Fontaine, S., Barot, S., Barré, P., Bdioui, N., Mary, B., & Rumpel, C. (2007). Stability of organic carbon in deep soil layers controlled by fresh carbon supply. *Nature*, *450*(7167), 277–280. https://doi.org/10.1038/nature06275

Frantz, D. (2019). FORCE—landsat + sentinel-2 analysis ready data and beyond. *Remote Sensing*, *11*(9), 1124. https://doi.org/10.3390/rs11091124

Gaiser, T., Perkons, U., Küpper, P. M., Kautz, T., Uteau-Puschmann, D., Ewert, F., Enders, A., & Krauss, G. (2013). Modeling biopore effects on root growth and biomass production on soils with pronounced sub-soil clay accumulation. *Ecological Modelling*, *256*, 6–15. https://doi.org/10.1016/j.ecolmodel.2013.02.016

Gao, W., Hodgkinson, L., Jin, K., Watts, C. W., Ashton, R. W., Shen, J., Ren, T., Dodd, I. C., Binley, A., Phillips, A. L., Hedden, P., Hawkesford, M. J., & Whalley, W. R. (2016). Deep roots and soil structure. *Plant, Cell & Environment*, *39*, 1662–1668. https://doi.org/10.1111/pce.12684

Grosse, B. (1974). Ergebnisse eines 7-jährigen Versuches zur Erhöhung der Ertragsfähigkeit einer Parabraunerde aus Löss mit Hilfe des meliorativen Tiefumbruchs. Abhandl. 10. *Internationaler Bodenkundlicher Kongreß*, *4*, 270–279.

Han, E., Kirkegaard, J. A., White, R., Smith, A. G., Thorup-Kristensen, K., Kautz, T. [. T.]., & Athmann, M. [. M.]. (2022). Deep learning with multisite data reveals the lasting effects of soil type, tillage and vegetation history on biopore genesis. *Geoderma*, *425*, 116072. https://doi.org/10.1016/j.geoderma.2022.116072

Hartge, K. H. (1980). Mechanical limitations to successful amelioration of soil structure—Demonstrated on a deep ploughed loess parabraunerde (Udalf). *Soil & Tillage Research*, *1*, 187–194. https://doi.org/10.1016/0167-1987(80)90022-7

Holanda, F., Mengel, D. B., Paula, M. B., Carvaho, J. G., & Bertoni, J. C. (1998). Influence of crop rotations and tillage systems on phosphorus and potassium stratification and root distribution in the soil profile. *Communications in Soil Science and Plant Analysis*, *29*(15–16), 2383–2394. https://doi.org/10.1080/00103629809370118

Horn, R., Domżał, H., Słowińska-Jurkiewicz, A., & van Ouwerkerk, C. (1995). Soil compaction processes and their effects on the structure of arable soils and the environment. *Soil & Tillage Research*, *35*, 23–36. https://doi.org/10.1016/0167-1987(95)00479-C

Izumi, T., & Wagai, R. (2019). Leveraging drought risk reduction for sustainable food, soil and climate via soil organic carbon sequestration. *Scientific Reports*, *9*(1), 1–8. https://doi.org/10.1038/s41598-019-55835-y

Jastrow, J. D., Miller, R. M., & Boutton, T. W. (1996). Carbon dynamics of aggregate-associated organic matter estimated by carbon-13 natural abundance. *Soil Science Society of America Journal*, *60*(3), 801–807. https://doi.org/10.2136/sssaj1996.03615995006000030017x

Kautz, T., Amelung, W., Ewert, F., Gaiser, T., Horn, R., Jahn, R., Javaux, M., Kemna, A., Kuzyakov, Y., Munch, J. C., Pätzold, S., Peth, S., Scherer, H. W., Schloter, M., Schneider, H., Vanderborght, J., Vetterlein, D., Walter, A., Wiesenbeg, G. L. B., & Köpke, U. (2013). Nutrient aquisition from arable subsoils in temperate climates: A review. *Soil Biology & Biochemistry*, *57*, 1003–1022. https://doi.org/10.1016/j.soilbio.2012.09.014

Kehl, M., Eckmeier, E., Franz, S. O., Lehmkuhl, F., Soler, J., Soler, N., Reicherter, K., & Weniger, G.-C. (2014). Sediment sequence and site formation processes at the Arbreda Cave, NE Iberian Peninsula, and implications on human occupation and climate change during the last glacial. *Climate of the Past*, *10*(5), 1673–1692. https://doi.org/10.5194/cp-10-1673-2014

Krause, L., Rodionov, A., Schweizer, S. A., Siebers, N., Lehndorff, E., Klumpp, E., & Amelung, W. (2018). Microaggregate stability and storage of organic carbon is affected by clay content in arable Luvisols. *Soil & Tillage Research*, *182*, 123–129. https://doi.org/10.1016/j.still.2018.05.003

Lipiec, J., Horn, R., Pietrusiewicz, J., & Siczek, A. (2012). Effects of soil compaction on root elongation and anatomy of different cereal plant species. *Soil and Tillage Research*, *121*, 74–81. https://doi.org/10.1016/j.still.2012.01.013

Lipiec, J., & Simota, C. (1994). Role of soil and climate factors in influencing crop responses to soil compaction in central and Eastern Europe. In *Developments in agricultural engineering. Soil compaction in crop production* (Vol. 11, pp. 365–390). Elsevier. https://doi.org/10.1016/B978-0-444-88286-8.50024-6

Meyer, N., Welp, G., Rodionov, A., Borchard, N., Martius, C., & Amelung, W. (2018). Nitrogen and phosphorus supply controls soil organic carbon mineralization in tropical topsoil and subsoil. *Soil Biology and Biochemistry*, *119*, 152–161. https://doi.org/10.1016/j.soilbio.2018.01.024

Morari, F., Berti, A., Dal Ferro, N., & Piccoli, I. (2019). Deep carbon sequestration in cropping systems. *Sustainable Agriculture Reviews*, *29*, 33–65. https://doi.org/10.1007/978-3-030-26265-5_2

Murphy, J., & Riley, J. P. (1962). A modified single solution method for the determination of phosphate in natural waters. *Analytica Chimica Acta*, *27*, 31–36. https://doi.org/10.1016/S0003-2670(00)88444-5

Nawaz, M. F., Bourrié, G., & Trolard, F. (2013). Soil compaction impact and modelling. A review. *Agronomy for Sustainable Development*, *33*(2), 291–309. https://doi.org/10.1007/s13593-011-0071-8

Perkons, U., Kautz, T., Uteau, D., Peth, S., Geier, V., Thomas, K., Lütke Holz, K., Athmann, M., Pude, R., & Köpke, U. (2014). Root-length densities of various annual crops following crops with contrasting root systems. *Soil and Tillage Research*, *137*, 50–57. https://doi.org/10.1016/j.still.2013.11.005

Peters, W., Bastos, A., Ciais, P., & Vermeulen, A. (2020). A historical, geographical and ecological perspective on the 2018 European summer drought. *Philosophical Transactions of the Royal Society of Britain*, *375*(20190505), 1–8. https://doi.org/10.1098/rstb.2019.0505

Plaza-Bonilla, D., Cantero-Martínez, C., & Alvaro-Fuentes, J. (2010). Tillage effects on soil aggregation and soil organic carbon profile distribution under Mediterranean semi-arid conditions. *Soil Use and Management*, *26*, 465–474. https://doi.org/10.1111/j.1475-2743.2010.00298.x

Pöhlitz, J., Rücknagel, J., Schlüter, S., Vogel, H.-J., & Christen, O. (2020). Estimation of critical stress ranges to preserve soil functions for differently textured soils. *Soil and Tillage Research*, *200*, 104637. https://doi.org/10.1016/j.still.2020.104637

Ponder, F. (1981). Influence of soil mixing and sterilization on growth and nutrient uptake of black walnut seedlings. *Communications in Soil Science and Plant Analysis*, *12*(9), 881–896. https://doi.org/10.1080/00103628109367202

Querejeta, J. I., Ren, W., & Prieto, I. (2021). Vertical decoupling of soil nutrients and water under climate warming reduces plant cumulative nutrient uptake, water-use efficiency and productivity. *New Phytologist*, *230*, 1378–1393. https://doi.org/10.1111/nph.17258

R Core Team. (2022). *R: A language and environment for statistical computing* (version 4.2.0) [Computer software]. R Foundation for Statistical Computing. Vienna: Austria. https://www.R-project.org/

Riekerk, H. (1971). The mobility of phosphorus, potassium, and calcium in a forest soil. *Soil Science Society of America Journal*, *35*(2), 350–356. https://doi.org/10.2136/sssaj1971.03615995003500020047x

Rossato, L., Alvalá, R. C. D. S., Marengo, J. A., Zeri, M., Cunha, A. P. M. d. A., Pires, L. B. M., & Barbosa, H. A. (2017). Impact of soil moisture on crop yields over Brazilian semiarid. *Frontiers in Environmental Science*, *5*, 73. https://doi.org/10.3389/fenvs.2017.00073

Scheffer, K., & Meyer, B. (1970). Tiefumbruchversuch einer Löß-Parabraunerde – Zielsetzungen, Anlage, Bodenphysik, Phosphathaushalt, Humus-Haushalt, N- und K-Haushalt, Erträge u. Nährstoffaufnahme. *Göttinger Bodenkundliche Berichte*, *16*, 1–178.

Schittenhelm, S., Kraft, M., & Wittich, K.-P. (2014). Performance of winter cereals grown on field-stored soil moisture only. *European Journal of Agronomy*, *52*, 247–258. https://doi.org/10.1016/j.eja.2013.08.010

Schneider, F., & Don, A. (2019a). Root-restricting layers in German agricultural soils. Part I: Extent and cause. *Plant and Soil*, *442*, 433–451. https://doi.org/10.1007/s11104-019-04185-9

Schneider, F., & Don, A. (2019b). Root-restricting layers in German agricultural soils. Part II: Adaptation and melioration strategies. *Plant and Soil*, *442*, 419–432. https://doi.org/10.1007/s11104-019-04186-8

Schneider, F., Don, A., Hennings, I., Schmittmann, O., & Seidel, S. J. (2017). The effect of deep tillage on crop yield – What do we really know? *Soil & Tillage Research*, *174*, 193–204. https://doi.org/10.1016/j.still.2017.07.005

Schüller, H. (1969). Die CAL-Methode, eine neue Methode zur Bestimmung des pflanzenverfügbaren Phosphates in Böden. *Zeitschrift für Pflanzenernährung und Bodenkunde*, *123*(1), 48–63. https://doi.org/10.1002/jpln.19691230106

Sharpley, A. N. (2003). Soil mixing to decrease surface stratification of phosphorus in manured soils. *Journal of Envrionmental Quality*, *32*, 1375–1384. https://doi.org/10.2134/jeq2003.1375

Shen, X., Wang, L., Yang, Q., Xiu, W., Li, G., Zhao, J., & Zhang, G. (2021). Dynamics of soil organic carbon and labile carbon fractions in soil aggregates affected by different tillage managements. *Sustainability*, *13*, 1541. https://doi.org/10.3390/su13031541

Six, J., Elliot, E. T., Paustian, K., & Doran, J. W. (1998). Aggregation and soil organic matter accumulation in cultivated and native grassland soils. *Soil Science Society of America Journal*, *62*, 1367–1377. https://doi.org/10.2136/sssaj1998.03615995006200050032x

Six, J., Paustian, K., Elliott, E. T., & Combrink, C. (2000). Soil structure and organic matter I. Distribution of aggregate-size classes and aggregate-associated carbon. *Soil Science Society of America Journal*, *64*(2), 681–689. https://doi.org/10.2136/sssaj2000.642681x

Smucker, A., McBurney, S. L., & Srivastava, A. K. (1982). Quantitative separation of roots from compacted soil profiles by the hydropneumatic elutriation system. *Agronomy Journal*, *74*(3), 500–503. https://doi.org/10.2134/agronj1982.00021962007400030023x

Sun, M., Ren, A. X., Gao, Z. Q., Wang, P. R., Mo, F., Xue, L. Z., & Lei, M. M. (2018). Long-term evaluation of tillage methods in fallow season for soil water storage, wheat yield and water use efficiency in semiarid southeast of the Loess Plateau. *Field Crops Research*, *218*(24–32), 24–32. https://doi.org/10.1016/j.fcr.2017.12.021

Tisdall, J. M., & Oades, J. M. (1982). Organic matter and water-stable aggregates in soils. *Journal of Soil Science*, *33*(2), 141–163. https://doi.org/10.1111/j.1365-2389.1982.tb01755.x

Toreti, A., Belward, A., Perez-Dominguez, I., Naumann, G., Luterbacher, J., Cronie, O., Seguini, L., Manfron, G., Lopez-Lozano, R., Baruth, B., van den Berg, M., Detener, F., Ceglar, A., Chatzopoulos, T., & Zampieri, M. (2019). The exceptional 2018 European water seesaw calls for action on adaptation. *Earth's Future*, *7*, 652–663. https://doi.org/10.1029/2019EF001170

Vannoppen, A., Gobin, A., Kotova, L., Top, S., Cruz, L. d., Vīksna, A., Aniskevich, S., Bobylev, L., Buntemeyer, L., Caluwaerts, S., Troch, R. d., Gnatiuk, N., Hamdi, R., Reca Remedio, A., Sakalli, A., van de Vyver, H., van Schaeybroeck, B., & Termonia, P. (2020). Wheat yield estimation from NDVI and regional climate models in Latvia. *Remote Sensing*, *12*(14), 2206. https://doi.org/10.3390/rs12142206

Vlaminck, S., Kehl, M., Rolf, C., Franz, S. O., Lauer, T., Lehndorff, E., Frechen, M., & Khormali, F. (2018). Late Pleistocene dust dynamics and pedogenesis in southern Eurasia – Detailed insights from the loess profile Toshan (NE Iran). *Quaternary Science Reviews*, *180*, 75–95. https://doi.org/10.1016/j.quascirev.2017.11.010

Waters, A. G., & Oades, J. M. (1991). Organic matter in water-stable aggregates. In W. S. Wilson (Ed.), *Advances in soil organic matter research: The impact on agriculture and the environment* (pp. 163–174). Woodhead Publishing.

Webster, R., & Lark, R. M. (2019). Analysis of variance in soil research: Examining the assumptions. *European Journal of Soil Science*, *70*(5), 990–1000. https://doi.org/10.1111/ejss.12804

Wendel, A. S., Bauke, S. L., Amelung, W., & Knief, C. (2022). Root-rhizosphere-soil interactions in biopores. *Plant and Soil*, *475*, 253–277. https://doi.org/10.1007/s11104-022-05406-4

Zeng, Q., & Brown, P. H. (2000). Soil potassium mobility and uptake by corn under differential soil moisture regimes. *Plant and Soil*, *221*(2), 121–134. https://doi.org/10.1023/A:1004738414847

Zhao, P., Li, S., Wang, E., Chen, X., Deng, J., & Zhao, Y. (2018). Tillage erosion and its effect on spatial variations of soil organic carbon in the black soil region of China. *Soil and Tillage Research*, *178*, 72–81. https://doi.org/10.1016/j.still.2017.12.022

SUPPORTING INFORMATION

Additional supporting information can be found online in the Supporting Information section at the end of this article.

How to cite this article: Burger, D. J., Schneider, F., Bauke, S. L., Kautz, T., Don, A., & Amelung, W. (2023). Fifty years after deep-ploughing: Effects on yield, roots, nutrient stocks and soil structure. *European Journal of Soil Science*, *74*(6), e13426. https://doi.org/10.1111/ejss.13426